Application of a New Crystal Growth Inhibition Based KHI Evaluation Method to Commercial Formulation Assessment

Proceedings of the 7th International Conference on Gas Hydrates (ICGH 2011),
Edinburgh, Scotland, United Kingdom, July 17-21, 2011.

APPLICATION OF A NEW CRYSTAL GROWTH INHIBITION BASED KHI EVALUATION METHOD TO COMMERCIAL FORMULATION ASSESSMENT

Philippe Glénat*
TOTAL, Centre Scientifique et Technique Jean Feger
Avenue Larribau, 64018 Pau Cedex
FRANCE

Ross Anderson, Houra Mozaffar & Bahman Tohidi
HYDRAFACT Ltd. & Centre for Gas Hydrate Research
Heriot-Watt University
Edinburgh, EH14 4AS
UNITED KINGDOM

ABSTRACT

Low dosage Kinetic Hydrate Inhibitors (KHIs) have seen increasing use as a cost effective technology for gas hydrate control in the oil and gas industry, offering significant CAPEX/OPEX advantages over traditional thermodynamic inhibitors (e.g. methanol, glycols). As KHIs are traditionally considered 'nucleation inhibitors' – i.e. they extend the induction (or 'hold') time, t_i, at a specific subcooling before hydrate nucleation proceeds to growth – evaluation is typically undertaken by measurement t_i as a function of various parameters at the conditions of interest. However, as nucleation is stochastic by nature, obtaining repeatable/transferrable data is often highly problematic and time-consuming, making robust evaluation difficult. Likewise, the focus on nucleation, and associated belief that the appearance of hydrate crystals in a KHI inhibited system means the inhibitor has failed, lowers confidence in field use. Here, we discuss the application of a new crystal growth inhibition (CGI) based approach to evaluate a number of commercial formulations for a gas condensate system. As reported for simple gas−water−polymer systems in a companion paper, commercial KHI formulations similarly induce a number of highly repeatable, well-defined hydrate crystal growth inhibition regions as a function of subcooling, ranging from complete inhibition (even hydrate dissociation), through severely to moderately reduced growth rates, ultimately to final rapid/catastrophic growth as subcooling increases. Delineation of these regions provides a much more reliable and rapid means to evaluate the relative performance of KHIs under simulated worst case scenario conditions; i.e. hydrate already present. Furthermore, the ability of KHIs to completely or severely inhibit hydrate growth even when modest fractions of hydrate (e.g. 0.5% of water converted) are present gives greatly increased confidence in terms of real-world application. Significantly, while recommended by vendors for the systems under study, tested KHIs varied greatly in their ability to inhibit crystal growth, demonstrating the limitations of traditional t_i based test methods in providing a suitably robust evaluation protocol.

Keywords: gas hydrates, KHI, methane, propane, experimental data, crystal growth, inhibition

* Corresponding author: Phone: +33 559 83 67 13 Fax +33 559 83 42 99 E-mail: philippe.glenat@total.com

NOMENCLATURE

ΔT_{s-I}	Temperature difference from s-I hydrate phase boundary [°C]
ΔT_{s-II}	Temperature difference from s-II hydrate phase boundary [°C]
ΔP_h	Change in pressure due to hydrate formation [bar]
CI	Corrosion Inhibitor
CIR	Complete (hydrate) Inhibition Region
CGI	Crystal Growth Inhibition
KHI	Kinetic Hydrate Inhibitor
RFR	Rapid (KHI) Failure Region
RGR	Reduced (hydrate) Growth (rate) Region
SDR	Slow (abnormally, hydrate) Dissociation Region
SG	Second Germination (KHI test method)
t_i	Hydrate nucleation induction time [hrs]

INTRODUCTION

Low dosage Kinetic Hydrate Inhibitors (KHIs) have seen increasing use as a cost effective technology for gas hydrate control in the oil and gas industry, offering significant CAPEX/OPEX advantages over traditional thermodynamic inhibitors (e.g. methanol, glycols) [1-3]. The widespread understanding within industry and academia is that KHI polymers (e.g. PVCap, poly-n-vinylcaprolactam) delay/slow down/interfere with the process of hydrate nucleation by surface adsorption on nuclei [4-7], forcing in an increased 'induction' or 'hold' time, t_i; the time that passes at a specific subcooling (ΔT from the hydrate phase boundary at pressure, P) within the hydrate stability zone (HSZ) before critical nuclei are achieved and hydrate nucleation to proceeds to growth. In theory, if the KHI-induced induction time, t_i, at ΔT,P is greater than the pipeline fluid residence time at that condition, then the KHI should be able to prevent hydrate nucleation/growth, whereby avoiding plugging.

As KHIs are primarily considered 'nucleation inhibitors', they are generally developed and tested through laboratory induction/hold time studies [1-3]. The same applies for determining the effects of various parameters including pressure, presence of synergists, salts, liquid hydrocarbons (condensate, oil) and other oilfield chemicals (e.g. corrosion and scale inhibitors). However, there is an inherent problem induction time measurements; nucleation is very sensitive and probabilistic by nature, meaning test results are often highly stochastic and poorly transferable [1-3,8-12]. Furthermore, this tendency to focus on KHIs as nucleation inhibitors often leads to the mistaken impression that the moment a hydrate crystal appears in a KHI inhibited system, the inhibitor has failed. These issues have resulted in low operator confidence in KHIs, restricting uptake by the industry, even though they are now being used successfully in the field [1,2].

To overcome the problem of poor reproducibility of KHI tests, TOTAL developed – and used for a number of years – a specific procedure in their semi-industrial hydrate flow loops they termed the "Second Germination" (SG) method. This proved to be very efficient in their hydrodynamic, through tubing flowing test conditions [8]. The procedure was subsequently applied in 2006 to autoclave cells with respect to tackling the ongoing problem of stochasticity in laboratory KHI data [9]. In Duchateau et al. [10,11] (University of Pau in conjunction with TOTAL) this new SG test protocol was reported; with results supporting significant improvements over traditional approaches in terms of repeatability and transferability of KHI test results. In summary, the SG method involves forming first forming hydrate at high subcooling, then dissociating this hydrate before then re-cooling to measure t_i and/or the subcooling of hydrate formation at constant cooling rate. By maintaining the temperature close to the hydrate phase boundary during the dissociation step, it was concluded that 'nuclei' of some form – related to the phenomenon of 'hydrate history' – were preserved, and that these aided more consistent nucleation/growth patterns when re-cooling to form hydrate (i.e. the 'second germination'), resulting in much more repeatable data.

While the SG method undoubtedly offers significant benefits over traditional approaches – as supported by independent studies [12] – the underlying theory behind it raises some important questions. In particular, if the conclusions are correct in that the second hydrate formation process is strongly influenced by some form of preserved hydrate 'nuclei', then it is logical to ask how an apparent induction time could actually exist in a system with nuclei already present; i.e. why does hydrate not form immediately on re-cooling into the hydrate region if 'seeded'. Related to this are literature reports which describe

apparent complete KHI-induced hydrate growth inhibition in atmospheric pressure THF/ethylene oxide aqueous systems [13-15], and anomalously slow dissociation of hydrates in the presence of KHIs [16,17], which both suggest that KHI polymers are very active well beyond the nucleation phase of hydrate formation. Combined, the above prompted Anderson et al. [18] (discussed in the companion paper to this work) to examine the ability of KHIs to inhibit (and anomalously preserve) methane and natural gas hydrates in systems with small fractions of hydrate present, i.e. once the nucleation step was complete and the KHI should have 'failed' according to conventional wisdom. In effect, this was taking the second germination method one step further; the reasoning behind this being that, if KHIs were able to prevent nuclei becoming crystals, or delay this process significantly rather than inhibiting nucleation alone, then they may be able to do the same for viable crystals, as seemingly the case for THF and ethylene oxide. This was found to be the case, with results showing that far from being primarily 'nucleation inhibitors', KHI polymers are in fact very powerful crystal growth inhibitors, with this latter property being much simpler to reliably quantify as it is driven by primarily by thermodynamic processes (presumably crystal surface adsorption) rather than kinetic. These findings led to the development of a novel crystal inhibition (CGI) method for KHI evaluation, which was supported by the industry through a Joint Industry Project (JIP) at Heriot-Watt University, Scotland, UK.

In the companion paper to this work [18], the basis of the CGI approach and its development as a method for KHI evaluation is described. Here, we report the application of this new method to evaluate the relative hydrate inhibition performance of a number of commercial KHI + corrosion inhibitor (CI) formulations for a gas condensate system; the aim being to assess its suitability for KHI field evaluation studies.

EXPERIMENTAL

Equipment and Materials

All tests were conducted on in-house (Hydrafact / Heriot-Watt University) designed/built 280 ml volume high pressure (max 410 bar) titanium (salt compatible) autoclave cells, as illustrated in Figure 1. For these set-ups, cell temperature is controlled by circulating coolant from a programmable cryostat through a jacket surrounding cells. Temperature is determined by platinum resistance thermometers (PRT, ± 0.1 °C), with pressure measured by either strain standard gauge (± 0.07 bar) or precision *Quartzdyne* (± 0.0007 bar) transducers; these being regularly calibrated against a dead weight tester. Cell pressure and temperature are continually monitored and recoded by computer. Impeller speed was typically set at 750 rpm.

As noted, tests were carried out on a real (dead) gas condensate (Dolphin, Qatar) with a synthetic methane–propane (98 and 2 mole% respectively) gas mixture. The gas mixture was prepared gravimetrically with the composition checked by GC. Cell liquids volume fractions were 0.3 aqueous to 0.7 condensate in all tests (Table 1). The aqueous phase was 0.1 mass% NaCl with 1.5 mass% KHI and 0.12 mass% (1200 ppm) corrosion inhibitor added (CI) for KHI tests.

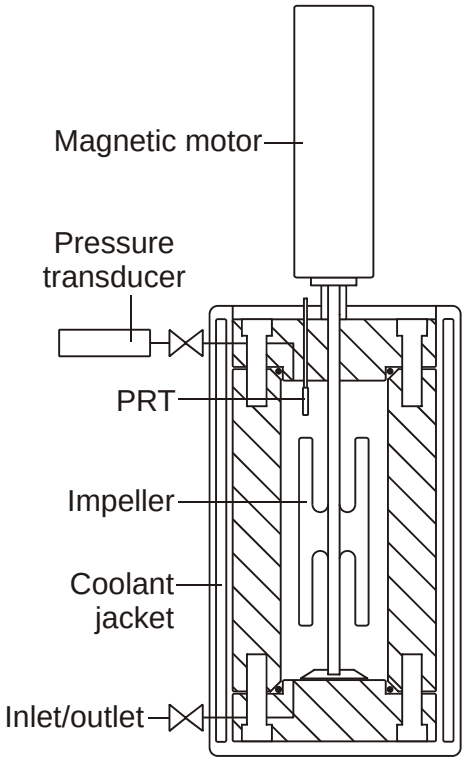

Figure 1. Schematic illustration of the 280 ml high pressure (max 410 bar) autoclave cells used in experiments.

	Initial Volume (ml)
Cell	280
Condensate	175
Aqueous	75
	Aqueous Concentration (mass%)
NaCl	0.1
KHI	1.5 or 0.0 (baseline tests)
CI	0.12

Table 1. Cell/fluid volumes, KHI and salt concentrations used in experiments.

	Typical growth rates order of magnitude (% water / hr)	Growth rate description
CIR	0.00	No growth
RGR (VS)	0.01 (< 0.05)	Very slow
(S)	0.1 (≥ 0.05 to < 0.5)	Slow
(M)	1 (≥ 0.5 to < 5)	Medium
RFR	10 (≥ 5) or as for KHI-Free system	Rapid
SDR	Dissociation rate one order of magnitude less than for no KHI	(Abnormally) Slow dissociation

Table 2. Classification of crystal growth inhibition (CGI) regions based on orders of magnitude change in hydrate growth rates (% water converted to hydrate per hour), as commonly observed across region boundaries. Defining characteristics of the hydrate slow dissociation region (SDR), which corresponds to the 'history' region are also shown.

9 anonymous (to Hydrafact / Heriot-Watt, who carried out the tests) commercial KHI+CI combinations – as provided by chemical vendors – were tested. Here, these are simply named KHI1+CI1 and so forth.

Procedures: Dissociation Point Measurement

Prior to tests in the presence of KHI+CI combinations, the gas hydrate dissociation point for the aqueous + condensate + gas system was determined using the isochoric equilibrium step-heating method of Tohidi et al. [19]. In this approach, following formation of hydrate at high subcooling – as indicated by pressure drop (due to gas consumption) at constant volume – the system temperature is raised in steps (typically 0.5 to 1.0 °C per step), with sufficient time given following each step for the equilibrium to be reached, as indicated by stable pressure. Only equilibrium points are used to determine the final dissociation point (on the phase boundary) through isochoric interpolation.

Procedures: CGI Methods

As discussed, the work described here involved applying the crystal growth inhibition (CGI) method developed by Anderson et al., as described in detail in the companion paper to this manuscript [18]. In summary, for tests described here, the following simple version of the CGI approach was applied to evaluate commercial KHI(+CI) performance for the aqueous + condensate + gas system:

1. The system was first cooled rapidly to a high subcooling to induce hydrate formation
2. Following initial rapid hydrate formation, the system was then warmed in steps to dissociate most of the hydrate formed, leaving only a small fraction remaining (typically < 0.5% of water converted), while assessing the extent of any anomalously slow dissociation behaviour
3. Cell temperature was then reduced again at a constant cooling rate (typically 1.0 °C / hr) to observe clear changes in growth rate as a function of subcooling
4. Steps 2-3 were repeated a number of times (2-3 where appropriate) to examine repeatability
5. Finally, following a repeat of Step 2 (after 3), the system was step-cooled with a small fraction of hydrate present to confirm the extent of the complete inhibition and very slow growth regions where appropriate

From PT data generated during the above steps, changes in relative growth rates were used to delineate obvious changes in KHI-induced crystal growth inhibition regions, allowing mapping and description of these regions for comparative KHI+CI combination evaluation. Similar procedures were also carried out on the KHI-free baseline system to provide appropriate growth rate data to compare with KHI system results. In all cases, the fraction of hydrate present was calculated from system composition and volumetric data using the in-house HydraFLASH® thermodynamic model [20].

With respect to the CGI method, while identification of clear changes in growth rate at particular subcoolings is generally straightforward, classification within defined regions according to growth rate – a 'relative' property – is not as simple. Table 2 shows the classification approach adopted here, as discussed in Anderson et al. [18].

In summary, the properties of the complete inhibition (CIR) and rapid failure regions (RFR) can be very specifically defined; for the former, growth is indefinitely inhibited (with potential hydrate dissociation) and in the latter, growth is at least equal to that for the same system in the absence of a KHI. Likewise the region where reduced growth rate (RGR) is observed can be simply defined as 'growth being slower than the KHI-free system' for the same PTX conditions. However, subdivision of the RGR – which has proven important given the wide range of inhibited growth rates observed – requires some specification of actual/relative growth rates. For simplicity, a growth rate order of magnitude classification has been adopted, which is deemed appropriate based on results to date and the obvious apparent relationship between CGI regions and exponential-like induction time trends, as described by Anderson et al. [18].

As an example a growth rate of 0.03% water converted per hour would be 'very slow' (VS), 0.07% / hr would be slow (S) and 0.6% / hr would be medium (M), so long as the value is less than that for the no KHI case. If the value is equal to that for no KHI, behaviour is classed as RFR (rapid failure), i.e. the KHI is failing to appreciably inhibit hydrate growth.

RESULTS AND DISCUSSION

As discussed, tests were carried out on a baseline (no KHI/CI) system before the effects of the 9 different KHI+CI combinations were examined using the CGI method. Results for the baseline and KHI+CI systems – with focus on 3 of the KHI+CI systems as examples – are discussed below.

KHI/CI-Free Baseline System

Prior to KHI+CI combination testing, phase equilibria and typical hydrate growth rates/patterns for the KHI/CI-free aqueous–condensate–gas system were examined using the procedures described in the previous section. Figure 2 shows a PT plot of raw cooling/step heating data, extracted equilibrium points and interpolations to determine the s-II dissociation point for the baseline system. As discussed, the gas mixture used in tests was 98 mole% methane / 2 mole% propane. However, due to preferential propane dissolution into the condensate, the actual composition of the gas phase in equilibrium with hydrate on the phase boundary corresponds to 0.85 mole% propane, as shown in Figure 2 when compared to HydraFLASH® model predictions.

Figure 3 shows example cooling and heating curves for the blank (no KHI/CI) aqueous + condensate + gas system plotted as pressure drop due to hydrate formation (ΔP_h) versus subcooling from the s-II hydrate phase boundary ($\Delta T_{s\text{-}II}$).

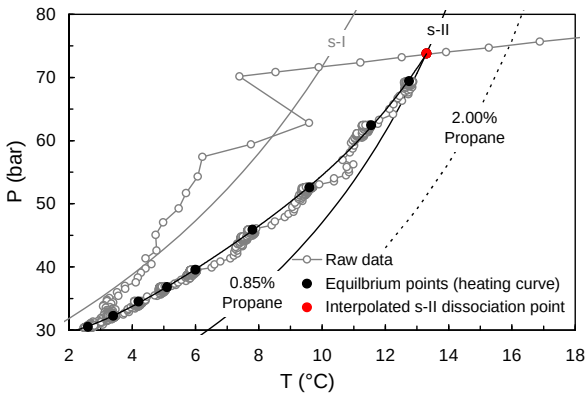

Figure 2. PT plot of raw cooling/step heating data, determined equilibrium points and interpolation for s-II dissociation point for the baseline (no KHI/CI) aqueous + condensate + gas system.

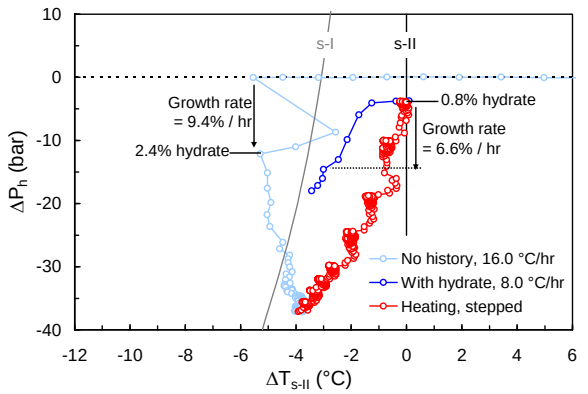

Figure 3. Example cooling and heating curves for the baseline (no KHI/CI) aqueous + condensate + gas system plotted as pressure drop due to hydrate formation (ΔP_h) versus subcooling from the s-II hydrate phase boundary ($\Delta T_{s\text{-}II}$).

As can be seen, for no history present, nucleation initiates at a subcooling of ~5.5 °C, with ~2.35% of water being converted to hydrate within 15 minutes; this corresponding to a hydrate growth rate of ~9.4% water converted per hour, as illustrated in Figure 4. Given that the system is condensate-dominated, this growth rate seems appropriate given gas supply to the aqueous phase water would be expected to be via diffusion from the gas head through the condensate to suspended water droplets.

During step-heating, dissociation occurs readily, with no anomalous preservation (Figure 3). As shown in Figure 4, when heated outside the hydrate region, hydrate quite readily dissociates as would be expected at a rate of 2.7% per hour initially.

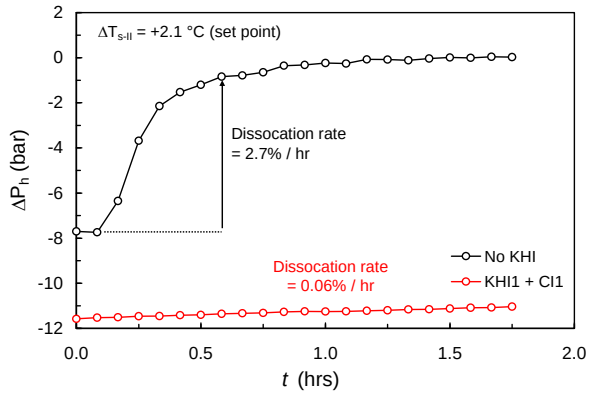

Figure 4. Plot of pressure drop due to the presence of hydrate (ΔP_h) versus time during dissociation at a temperature 2.1 °C outside the hydrate region for the aqueous + condensate + gas system with and without KHI1+CI1 present.

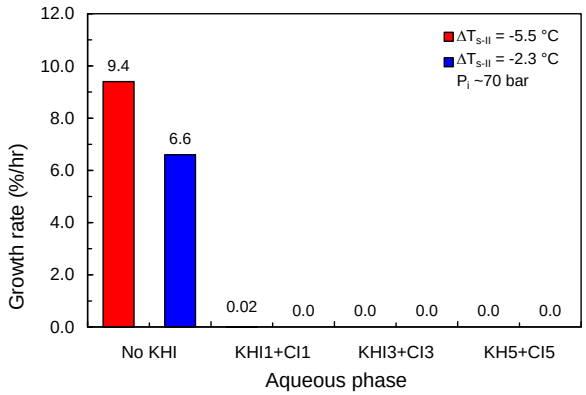

Figure 5. Plot of average initial hydrate growth rate (% water converted to hydrate per hour) for the blank and KHI systems at 2.3 and 5.5 °C subcoolings.

As illustrated in Figures 3 and 5, when re-cooling with a small fraction of hydrate still present (0.8 % of water as hydrate), growth begins in earnest effectively immediately at low subcoolings, as would be expected thermodynamically for a KHI-free, well mixed system.

KHI1 + CI1 Example Results

Figure 6 shows a PT plot of example CGI method cooling and heating curves with interpreted CGI region boundaries for KHI1+CI1. Figure 7 shows the same data plotted as ΔP_h versus $\Delta T_{s\text{-}II}$. Figure 8 shows ΔP_h and $\Delta T_{s\text{-}II}$ data for the step cooling run on this system with hydrate present as a function of time.

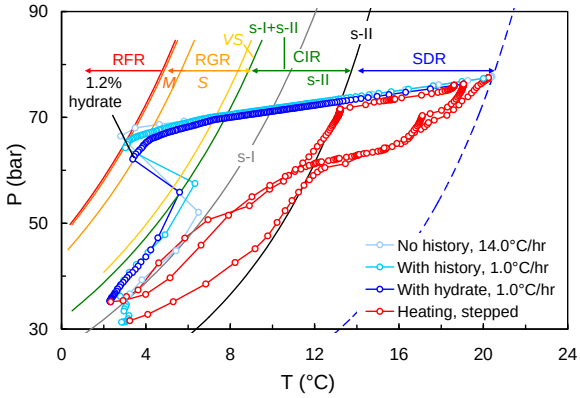

Figure 6. PT plot of example CGI method cooling and heating curves with interpreted CGI region boundaries for KHI1+CI1.

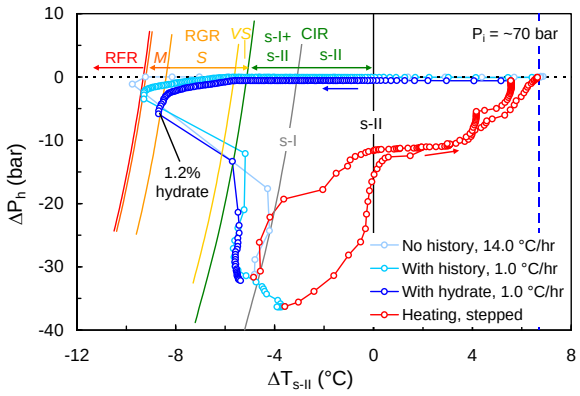

Figure 7. Example CGI method cooling and heating curves with interpreted CGI region boundaries for KHI1+CI1 plotted as pressure drop due to hydrate formation (ΔP_h) versus subcooling from the s-II hydrate phase boundary ($\Delta T_{s\text{-}II}$).

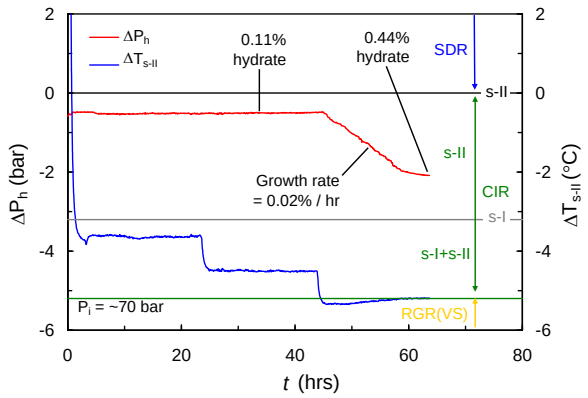

Figure 8. Pressure drop due to hydrate formation (ΔP_h) and subcooling from the s-II hydrate phase boundary ($\Delta T_{s\text{-}II}$) data for the step cooling run with hydrate present for the KHI1+CI1 system plotted as a function of time.

As can be seen, the KHI1+CI1 combination showed good hydrate crystal growth inhibition performance up to a subcooling of ~9.3 °C, beyond which rapid growth (RFR region) occurred suddenly, with growth rates becoming comparable with the KHI-free system. When cooling with small fractions of hydrate present (> 0.4 %), at cooling rates of 1.0 °C / hr, no obvious growth could be observed up to a subcooling of ~5.8 °C. Beyond this, a region of slow growth followed by a region of moderate growth was observed; these apparently being present up to concentrations of ~1.0% water as hydrate.

Step cooling with hydrate present revealed that complete inhibition (CIR) actually extended to ~5.2 °C subcooling at 70 bar, before very slow growth (RGR(VS)) initiated ahead of the obvious beginning of slow growth at ~5.8 °C subcooling. This is clearly shown in Figure 8; hydrate is present but does not grow for ~44 hours and 4.5 °C subcooling within the hydrate region. Only when the temperature is reduced to give 5.3 °C subcooling is very slow growth (0.02 % / hr) observed, with this growth halting again as pressure decrease due to hydrate formation causes PT conditions to re-enter the CIR.

The strong absorbance of the KHI1 polymer on crystal surfaces is reflected in a large anomalously slow dissociation region (SDR). As shown in Figures 4, at the same temperature (and final equilibrium pressure) outside the hydrate region, the dissociation rate for the polymer–hydrate complex formed in the KHI system is an order of magnitude less than that for the KHI-free system, even though there is more hydrate present.

KHI3 + CI3 Example Results

Figure 9 shows a PT plot of example CGI method cooling and heating curves with interpreted CGI region boundaries for KHI3+CI3 tests. Figure 10 shows the same data plotted as ΔP_h versus $\Delta T_{s\text{-}II}$. Figure 11 shows ΔP_h and $\Delta T_{s\text{-}II}$ data for the step cooling run with hydrate present as a function of time.

As can be seen, the KHI3+CI3 combination shows a similar total CGI subcooling extent as KHI1+CI1 at ~9.0 °C, beyond which sudden rapid growth consistently takes place if hydrate is present (and in this case for no hydrate history / first cooling).

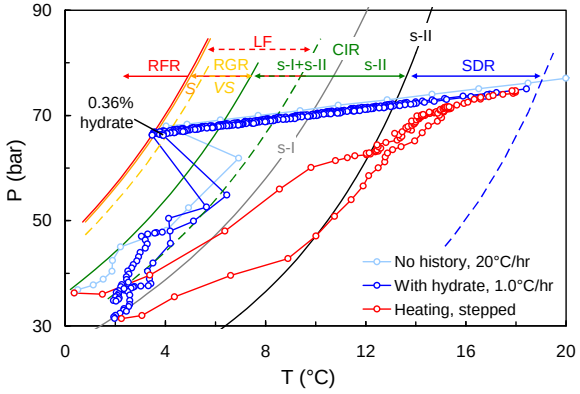

Figure 9. PT plot of example CGI cooling and heating curves with interpreted CGI region boundaries for KHI3+CI3.

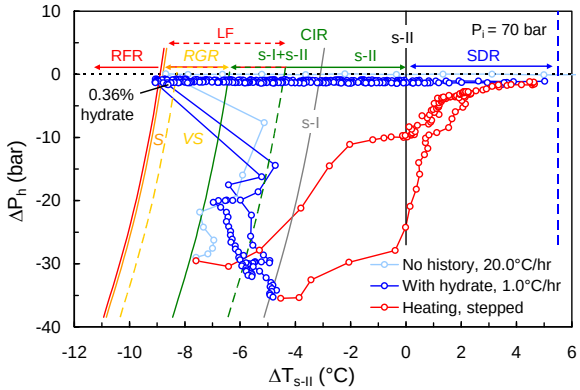

Figure 10. Example CGI cooling and heating curves with interpreted CGI region boundaries for KHI3+CI3 plotted as ΔP_h versus $\Delta T_{s\text{-}II}$.

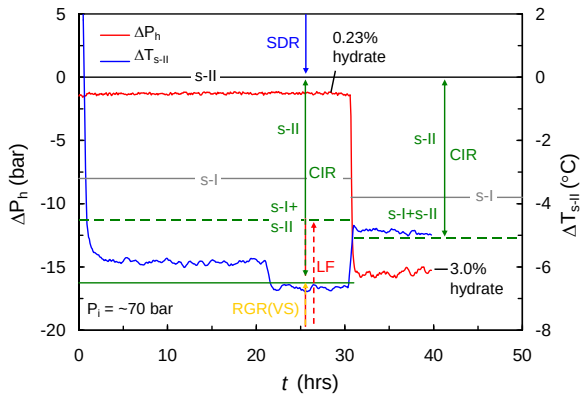

Figure 11. ΔP_h and $\Delta T_{s\text{-}II}$ data for the step cooling run with hydrate present for the KHI3+CI3 system plotted as a function of time.

However, the extent and nature of CGI region subdivisions is quite different. For KHI3+CI3, the region of complete inhibition (CIR) extends to a subcooling of ~6.4 °C, compared to ~5.2 °C for KHI1+CI1. The extent of the CIR for KHI3+CI3 is clear from step-cooling data (Figure 11). For the first step, at a subcooling of 5.8 °C, ΔP_h remains stable / the hydrate fraction unchanged for ~20 hrs. When the subcooling is increased by ~1.0 °C into the RGR(VS) region, only then is ΔP_h / the hydrate fraction seen to very slowly increase over the next 5 hours.

Following the CIR, a region of very slow growth extends to $\Delta T_{s\text{-}II}$ = ~–8.3 °C before growth rates start to increase slightly (RGR(S)) ahead of final rapid failure at $\Delta T_{s\text{-}II}$ = ~–9.0 °C. Thus KHI3+CI3 appears to offer superior performance compared with KHI1+CI1. However, this performance is limited to very low hydrate fractions (LF), as illustrated in Figure 10; sudden rapid failure occurred at hydrate fractions in excess of ~0.3% water converted to hydrate. This contrasts results for KHI1+CI1 which suggest CGI regions are retained up to ~1.0% water as hydrate at comparable subcoolings (> 8.0 °C) before sudden, rapid growth occurs (Figures 6 and 7).

Interestingly, in both no history and hydrate present cooling runs, following rapid failure, growth rates suddenly reduce at a similar subcooling (~1.3 °C) from the s-I phase boundary for the system (dashed green line in Figures 9 and 10), suggesting that part of the CIR is retained to higher hydrate fractions. This behaviour is consistent with CGI region boundaries paralleling the s-I boundary for the system, suggesting s-I hydrate formation is responsible for KHI failure.

For KHI3+CI3, anomalously slow dissociation was observed up to at least ~5.5 °C above the hydrate phase boundary, which is typical for strongly crystal surface adsorbing polymers in s-II forming systems.

KHI5 + CI5 Example Results

Figure 12 shows a PT plot of example CGI method cooling and heating curves with interpreted CGI region boundaries for KHI5+CI5. Figure 13 shows the same data plotted as ΔP_h versus $\Delta T_{s\text{-}II}$. Figure 14 shows ΔP_h and $\Delta T_{s\text{-}II}$ data for the step cooling run on with hydrate present as a function of time.

As can be seen, the CGI behaviour for this KHI/CI combination is quite different for KHI1+CI1 and KH13+CI3. For KHI5+CI5, there is effectively only one CGI region; the complete inhibition region (CIR) which extends to ~6.9 °C subcooling.

Following this, moderate growth rates drive PT conditions to track along the boundary between this region and the rapid failure region (RFR) where KHI influence on growth rates is negligible.

Complete hydrate growth inhibition is clearly evident in step-cooling with hydrate present data (Figure 13); over the first 87 hours / 3 steps to 5.8 °C subcooling not only does hydrate not grow, but it dissociates (ΔP_h reduces) on the initial step.

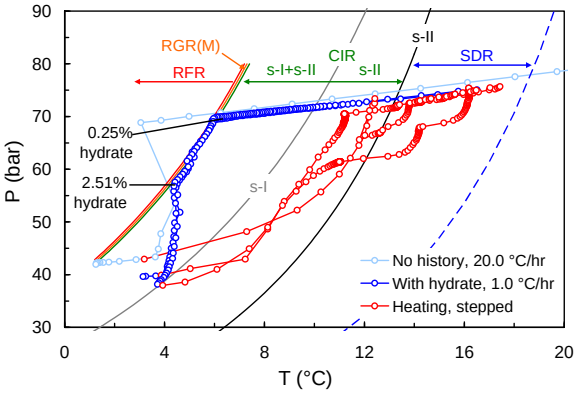

Figure 12. PT plot of example CGI method cooling and heating curves with interpreted CGI region boundaries for KHI5+CI5.

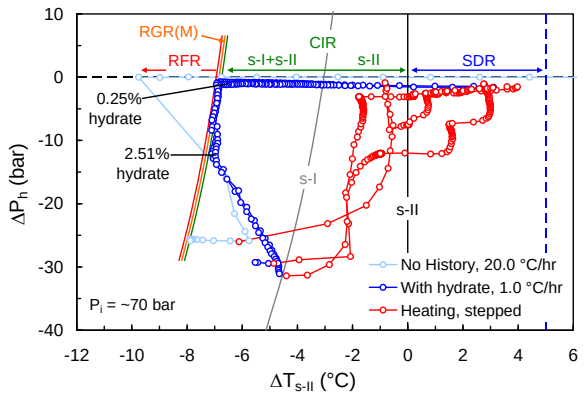

Figure 13. Example CGI cooling and heating curves with interpreted CGI region boundaries for KHI5+CI5 plotted as ΔP_h versus $\Delta T_{s\text{-}II}$.

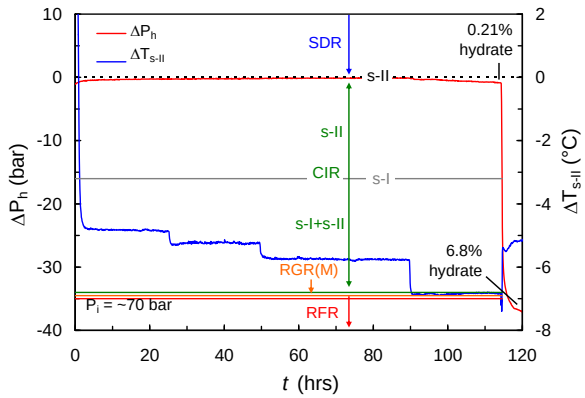

Figure 14. ΔP_h and $\Delta T_{s\text{-}II}$ data for the step cooling run with hydrate present for the KHI5+CI5 system plotted as a function of time.

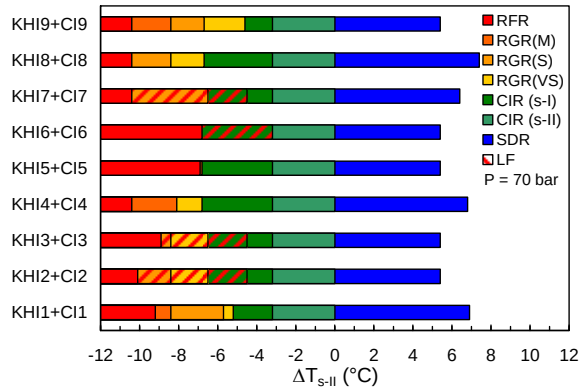

Figure 15. Experimentally determined KHI-induced gas hydrate crystal growth inhibition (CGI) regions for the 9 commercial KHI + CI combinations tested plotted as a function of total subcooling extent at 70 bar pressure. LF indicates that sudden, rapid failure can occur at low hydrate fractions (<~0.5% water as hydrate in this case).

Only when the subcooling is increased to just outside the CIR does growth increase to moderate rates as PT conditions follow the CIR/RFR boundary region with further cooling.

While the complete crystal growth inhibition subcooling extent of KHI5+CI5 is lower than that for KHI1+CI1 and KHI3+CI3, this is made up for by the fraction of hydrate it can tolerate before failure. As noted, and can be seen in Figures 13 and 14, it is apparently able to maintain complete crystal growth inhibition up to ~2.5% water converted to hydrate. Only past this fraction do PT conditions stop appreciably tracking the boundary region between the complete inhibition and rapid growth regions. As for KHI/CI combinations 1 and 5, behaviour is consistent with CGI region boundaries paralleling the s-I phase boundary for the system, again suggesting s-I hydrate formation is responsible for KHI.

For KHI5+CI5, anomalously slow dissociation was observed up to at least ~5.5 °C above the hydrate phase boundary, which is typical for strongly adsorbing polymers in s-II forming systems.

KHI+CI 1-9 Results Comparison

Figure 15 shows experimentally determined KHI-induced gas hydrate crystal growth inhibition (CGI) regions for all 9 commercial KHI + CI combinations tested (including those discussed as examples) plotted as a function of total subcooling extent from the s-II phase boundary at 70 bar pressure. As can be seen, all show distinct CGI regions, ranging from complete inhibition, through reduced growth rates, to ultimate rapid failure (growth rates as for an uninhibited system) as subcooling increases. However, even though the inhibitors were specifically selected as potential options for this gas condensate system – presumably following traditional KHI testing by vendors – inhibition performance varies considerably between the different KHI + CI combinations in both total CGI subcooling extent and degree of inhibition within individual regions. What does tie results for the different systems together is that many share common boundary positions as function of subcooling, although the nature of regions that these boundaries separate (CIR, RGR, RFR) varies.

As discussed in Anderson et al. [18], CGI studies to date strongly suggest KHI failure in multicomponent s-I/s-II forming systems (e.g. natural gases) is apparently due to the initial formation of s-I gas hydrates; CGI boundaries typically mirroring the s-I boundary in subcooling extent rather than the s-II boundary. The results of this study support this theory in that all KHI+CI combinations show complete inhibition (CIR) at least up to the s-I phase boundary for the system, with only the s-I + s-II complete inhibition region varying in extent in individual cases.

With respect to common region boundary positions, for example, KHI+C1 2, 3, 7, 9 all show a common boundary at ~1.3 °C subcooling from the s-I boundary (4.5 °C from s-II boundary).

For KHI+CI 9, this represents the limit of the CIR region, while for 2-3 and 7 CIR is retained, but only for low fractions of hydrate. Likewise, KHI+CI 2-9 all show a CGI boundary at ~3.5 °C subcooling from the s-I phase boundary (~6.8 °C subcooling from the s-II boundary). For KHI+CI 5-6, this marks the limit of appreciable crystal growth inhibition (CIR in these cases), while for 2-4 and 6-8 it delineates the change from complete inhibition to reduced growth rates. Further common boundaries occur at $\Delta T_{s\text{-}I}$ = −5.2 °C ($\Delta T_{s\text{-}II}$ = −8.4 °C) and $\Delta T_{s\text{-}I}$ = −7.1 °C ($\Delta T_{s\text{-}II}$ = −10.3 °C); the latter being the maximum limit of appreciable crystal growth inhibition out of all those KHI+CI combinations tested. This similarity in positioning of CGI boundaries as a function of subcooling supports the suggestion of Anderson et al. that this is related to underlying changes in natural crystal growth patterns as a function of subcooling (e.g. favoured faces, morphologies) upon which the KHI is acting.

In addition, results show that the fraction of water converted to hydrate to which the KHI can still offer good inhibition varies considerably. For example, while KHI 2 has a high total CGI extent, much of this only applies at low hydrate fractions (~0.3% hydrate), which when exceeded, results in sudden rapid hydrate growth (e.g. as seen in KHI3+CI3 detailed example data). In contrast, KHI1+CI CGI regions appeared to remain up to ~1.0 % hydrate, although the extent of the CIR and RGR(VS) was considerably reduced for this KHI. Likewise, while KHI5+CI5 could seemingly retain CGI properties to 2.5 % water converted to hydrate, this KHI was disadvantaged by a low total CGI subcooling extent. The simplest explanation for the varying fractions of hydrate these KHI formulations can tolerate would be varying polymer concentrations; the greater the polymer content, the greater the fraction of hydrate tolerated before the polymer is used up and the remaining aqueous concentration becomes insufficient to offer further significant crystal growth inhibition. The presence of more than one polymer (e.g. a weaker and a stronger absorbing) in different fractions could also potentially alter hydrate fraction tolerance as a function of subcooling.

As discussed by Anderson et al. [18], CGI data can also be used to estimate induction time patterns; with minimum t_i being zero just inside the RFR and rising exponentially to infinity as the RGR(VS) is entered/CIR approached. This, combined with the high degree of post-nucleation crystal growth inhibition revealed by the CGI method can allow much more confident selection of KHIs. For example, assuming an operating temperature of 4 °C ($\Delta T_{s\text{-}II}$ = −8.4 °C) at 70 bar, then from the data in Figure 15 the 9 KHI+CI combinations tested could be simply ranked in terms of total performance from best to worst as follows: 8, 9, 1, 2, 3, 7, 5, 6; this ranking taking the ability to handle on low fractions of hydrate into account (negative property).

While of course there are many other factors which help decide the most suitable KHI (e.g. thermal stability, cloud point, emulsion tendency, biodegradability), a basic CGI test (constant cooling with hydrate present) – which is similar to the second germination method but typically better in terms of repeatability due to the presence of actual hydrate crystals – carried out overnight provides a rapid method for screening (e.g. the early failure of 5 and 6 was obvious from the first runs) ahead of more detailed tests to determine all CGI boundaries/the specific nature of individual regions (CIR, RGR). The most promising candidates can then be assessed with respect to induction times; the CGI data providing a guide to the patterns expected, saving time and allowing wasted experiments to be avoided (i.e. if the subcooling is within the CIR region, then t_i is infinite, so a measurement is unnecessary).

Above all, the method is highly repeatable and gives both the testing laboratory and KHI user increased confidence. For example, if the results of CGI tests show at a given subcooling, a KHI can handle up to 0.5% hydrate before rapid/uninhibited growth, and hydrate will grow only at 0.05% / hour up to this fraction, then that could be considered a further 10 hours of potential protection in addition to any induction time. At such growth rates (RGR(S)), induction times of at least similar magnitude (10 hours) could be expected, giving a primary protection before CGI secondary protection in terms of hydrate formation/plugging.

The above of course assumes that hydrate particles are being carried by the liquid (aqueous or hydrocarbon) phase and are not adhering to pipeline surfaces, thus they are eventually carried out of the hydrate region as they move downstream. To date, in the RGR/CIR, results suggest that hydrates do primarily remain suspended within liquid phase as a fine particle suspension, although this requires further investigation.

CONCLUSIONS

In the companion paper to this work [18], a new crystal growth inhibition (CGI) approach for KHI evaluation was described. Here, we applied this new method to evaluate the relative hydrate inhibition performance of a number of commercial KHI + corrosion inhibitor (CI) formulations for an s-II forming gas condensate system.

As found for gas−water−base polymer systems in the companion paper, commercial KHI formulations similarly induce a number of highly repeatable, well-defined hydrate crystal growth inhibition regions as a function of subcooling, ranging from complete inhibition (even hydrate dissociation), through severely to moderately reduced growth rates, ultimately to final rapid/catastrophic growth as subcooling increases. Delineation of these regions provides a much more reliable and rapid means to evaluate the relative performance of KHIs under simulated worst case scenario conditions; i.e. hydrate already present. The method also yields an approximate expected induction time trend, allowing this data to be generated more efficiently.

Finally, the new CGI approach demonstrates the ability of KHIs to completely or severely inhibit hydrate growth even when modest fractions of hydrate (e.g. 0.5% of water converted) are present, giving a second line of protection (after any induction time) thus further increased operator confidence in terms of KHI field application.

REFERENCES

[1] Kelland MA. *History of the development of low dosage hydrate inhibitors*. Energy and Fuels 2006;20:825-847.

[2] Klomp U. *The world of LDHI: From conception to development to implementation*. Proceedings of the 6th International Conference on Gas hydrates, Vancouver, Canada, 2008:5409.

[3] Sloan ED, Koh CA. *Clathrate Hydrates of Natural Gases* (3rd ed.). Taylor & Francis / CRC Press, Boca Raton, FL, 2008.

[4] Freer EM, Sloan ED. *An engineering approach to kinetic inhibitor design using molecular dynamics simulations*. Annals of the New York Academy of Sciences, 2000;912:651-657.

[5] Makogon YM, Sloan ED. *Mechanism of kinetic hydrate inhibitors*. Proceedings of the 4th International Conference on Gas Hydrates, Yokohama, Japan 2002:498-503.

[6] Anderson BJ, Tester JW, Borghi GP, Trout B L. *Properties of inhibitors of methane hydrate formation via molecular dynamics simulations*. Journal of the American Chemical Society, 2005; 127:17852-17862.

[7] Kvamme B, Kuznetsova T, Aasoldsen K. *Molecular dynamics simulations for selection of kinetic hydrate inhibitors*. Journal of Molecular Graphics and Modelling 2005;23:524-536.

[8] Peytavy J-L, Glénat P, Bourg P. *Qualification of low dose hydrate inhibitors (LDHIs): field cases studies demonstrate the good reproducibility of the results obtained from flow loops*. Proceedings of the 6th International Conference on Gas hydrates, Vancouver, Canada, 2008:5499

[9] Duchateau C, Dicharry C, Peytavy J-L, Glénat P, Pou T-E, Hidaldo E. *Laboratory evaluation of kinetic hydrate inhibitors: a new procedure for improving the reproducibility of measurements*. Proceedings of the 6th International Conference on Gas hydrates, Vancouver, Canada, 2008:5582

[10] Duchateau C, Peytavy J-L, Glénat P, Pou T-E, Hidalgo M, Dicharry C. *Laboratory evaluation of kinetic hydrate inhibitors: A procedure for enhancing the repeatability of test results*. Energy and Fuels 2009;23(2):962-966.

[11] Duchateau C, Glénat P, Pou, T-E, Hidalgo M, Dicharry C. *Hydrate precursor test method for the laboratory evaluation of kinetic hydrate inhibitors*. Energy Fuels 2010;24:616–623.

[12] Ajiro A, Takemoto Y, Akashi M, Chua PC, Kelland MA. *Study of the Kinetic Hydrate Inhibitor Performance of a Series of Poly(N-alkyl-N-vinylacetamide)s.* Energy & Fuels 2010; 24(12);6400–6410.

[13] Makogon TY, Larsen R, Knight CA, Sloan ED. *Melt growth of tetrahydrofuran clathrate hydrate and its inhibition: Method and first results*. Journal of Crystal Growth 1997;179:258-262.

[14] Larsen R, Knight CA, Sloan ED. *Clathrate hydrate growth and inhibition*. Fluid Phase Equilibria 1998;150-151:353-360.

[15] Larsen R, Knight CA, Rider KT, Sloan ED. *Melt growth and inhibition of ethylene oxide clathrate hydrate*. Journal of Crystal Growth 1999;204:376-381.

[16] Habetinova E, Lund A, Larsen R. *Hydrate dissociation under the influence of low-dosage kinetic inhibitors*. Proceedings of the 4th International Conference on Gas Hydrates, Yokohama, Japan, 2002.

[17] Svartaas TM, Gulbrandsen AC, Huseboe SBR, Sandved O. *An experimental study on "un-normal" dissociation properties of structure II hydrates formed in presence of PVCAP at pressures in the region 30 to 175 bars – dissociation by temperature increase*. Proceedings of the 6th International Conference on Gas Hydrates, Vancouver, Canada, 2008:5696.

[18] Anderson R, Mozaffar H, Tohidi, B. *Development of a crystal growth inhibition based method for the evaluation of kinetic hydrate inhibitors.* Proceedings of the 7th International Conference on Gas Hydrates, Edinburgh, UK, 2011.

[19] Tohidi B, Burgass RW, Danesh A, Østergaard KK, Todd AC. *Improving the accuracy of gas hydrate dissociation point measurements.* Annals of the New York Academy of Sciences 2000;912(1):924-931.

[20] *HydraFLASH Model V2.2.* Hydrafact Ltd: Edinburgh, UK, 2011. www.hydrafact.com.

ACKNOWLEDGEMENTS

This work was funded by TOTAL Centre Scientifique et Technique Jean Feger, Pau, France. Experimental work was carried out by Hydrafact Ltd., Edinburgh; a Heriot-Watt University spin-out company.